Eclipse Pulsed Laser Deposition for Damage-Free Preparation of Transparent ZnO Electrodes on Top of Organic Solar Cells

Sylvio Schubert, Florian Schmidt, Holger von Wenckstern, Marius Grundmann, Karl Leo, and Lars Müller-Meskamp**

Pulsed laser deposited gallium doped zinc oxide (ZnO:Ga) is reported as transparent top electrode for organic solar cells. In contrast to standard coating techniques, prone to harm organic sublayers and leading to strongly reduced device efficiencies, eclipse pulsed laser deposition (PLD) in argon atmosphere is identified as compatible, nonharmful deposition method for ZnO:Ga, even on top of sensitive organic material. Although PLD is not yet ready for mass production, the experiments reveal and solve crucial process limitations, e.g., droplet impacts, which might be useful also for high yield deposition methods. Optimized ZnO:Ga top electrodes achieve a high mean transparency in the visible spectral range of T_{vis} = 82.7% and a reasonable sheet resistance of R_S = 83 Ω sq^{-1}. The organic photovoltaic devices prepared with this electrode obtained an efficiency of η = 2.9%, almost equal to the efficiency of reference samples using a state-of-the-art metal top contact (η = 3.0%). The investigations here demonstrate the successful deposition of transparent conductive oxides as top electrode for organic devices and open a new path towards the combination of metal oxides and organic semiconductors.

1. Introduction

Organic photovoltaics (OPV) are a highly promising technology for sustainable, individual, and cost-efficient on-site power generation.[1] Continuous advancements in material and concept development have led to significant improvements in device efficiency. Recently, a power conversion efficiency of 12% was realized by using a complex multijunction device architecture.[2] Such highly efficient devices, especially in the lab, commonly utilize indium tin oxide (ITO) as transparent bottom electrode on a glass substrate, because of its excellent optical and electrical properties with an average transmittance in the visible spectral range T_{vis} over 83% and a sheet resistance R_S down to 10 Ω sq^{-1}.[3] To avoid the high cost for indium,[4] zinc oxide (ZnO) is frequently used as electrode material in commercial applications. Upon extrinsic doping of ZnO with gallium or aluminum, sheet resistances below 20 Ω sq^{-1} are achieved at similar transparencies compared to ITO.[5] These properties render ZnO the electrode material of choice for inorganic thin-film solar cells and certainly a very interesting candidate for low-cost transparent electrodes of organic solar cells. Thus, we focused on the application of doped ZnO films as electrode on organic solar cells and compared them to reference devices with a thin metal electrode (**Figure 1**), which are commonly used to achieve efficient top-illuminated cells.

In order to be independent of a specific kind of substrate material (transparent or opaque) and to produce efficient semitransparent solar cells, a device architecture with highly transparent and sufficiently conductive top electrode is required, which allows a top illumination configuration of the device. For that purpose, ultrathin metal films,[6,7] metal nanowires,[8–10] carbon nanotubes,[11] graphene,[12] and C_{60}[13] are demonstrated. However, the application of doped ZnO, ITO, or other transparent conductive oxides as top electrode for small molecule organic semiconductor devices still faces several challenges: The required plasma-assisted deposition processes are known to degrade organic materials, leading to significantly reduced device efficiencies,[14,15] partially due to the release of UV light and radiation of higher energy. During deposition, a comparatively high partial pressure of oxygen is typically required, which strongly influences the layer conductivity but can harm the sensitive organic materials.[5,16] Furthermore, the maximum substrate temperatures during deposition and post annealing temperature are limited by the organic sublayers, resulting in unfavorable film morphology and reduced optoelectronic performance of the electrode itself.[17] Thus, organic solar cells with ZnO top electrode have not been reported so far. There are only a few publications dealing with other transparent

Dr. S. Schubert, Prof. K. Leo, Dr. L. Müller-Meskamp
Institut für Angewandte Photophysik (IAPP)
Technische Universität Dresden
George-Bähr-Str. 1, 01069 Dresden, Germany
E-mail: leo@iapp.de; lars.mueller-meskamp@iapp.de
Dr. F. Schmidt, Dr. H. von Wenckstern,
Prof. M. Grundmann
Institut für Experimentelle Physik II – Halbleiterphysik
Universität Leipzig
Linnéstr. 5, 04103 Leipzig, Germany

DOI: 10.1002/adfm.201500569

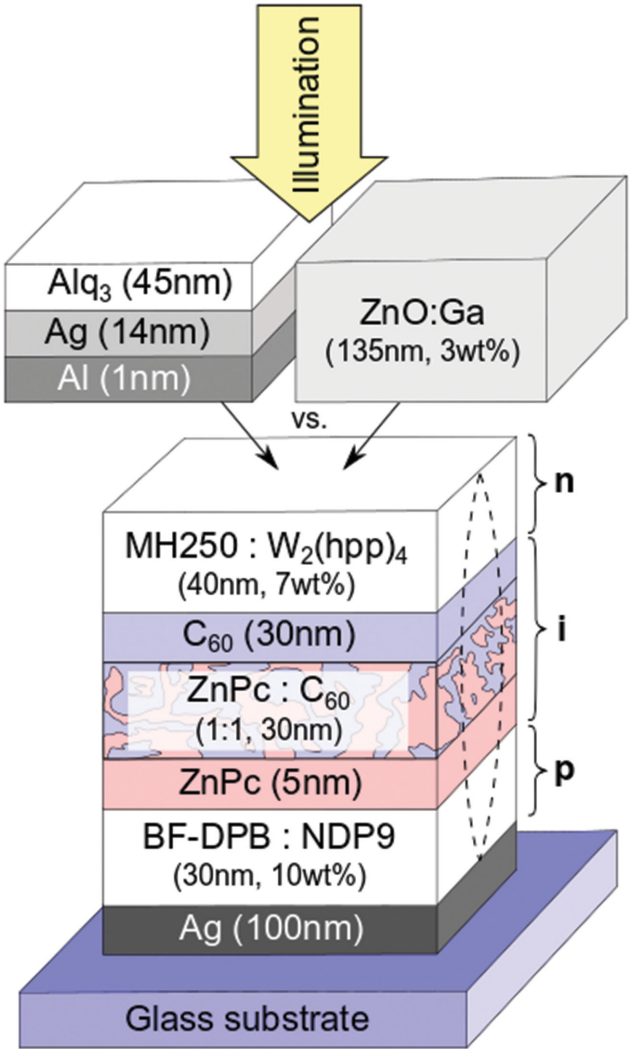

Figure 1. Schematic stack design of the top-illuminated p–i–n small molecule organic solar cells with eclipse pulsed laser deposited ZnO:Ga top electrode. A thermally evaporated state-of-the-art metal bilayer (Al/Ag) top electrode with Alq_3 capping is used as reference. The dashed lines indicate the optical field distribution inside the cell.

conductive oxides as top electrode for organic devices and the presented results are not easy to evaluate. Most of them demonstrate devices with sputter deposited ITO top electrodes and rather poor device efficiency η, e.g., organic solar cells with η = 0.7%.[14,15,18] However, a direct comparison of the electrodes shown in literature to our results is difficult due to the application of different organic materials.

Even though not free of drawbacks, pulsed laser deposition (PLD) is a low energy coating technique allowing the deposition of almost every oxide material or material combination with a typically stoichiometric transfer of the target composition to the thin film. For instance, gallium doped ZnO films with various doping concentrations can easily be realized by simply changing the mixing ratio of both materials in the target. Consequently, the layer conductivity can be strongly improved by appropriate doping.

Here, we demonstrate for the first time gallium doped zinc oxide (ZnO:Ga) thin films as top electrodes for efficient single-junction organic solar cells by using PLD in eclipse configuration at room temperature. After optimization of the ZnO:Ga electrode properties on single organic sublayers by varying the background gas atmosphere in the PLD chamber and the doping concentration, the best electrodes are deposited on top of complete organic solar cells. The origin of local shunt formation for standard PLD is investigated by thermography. Finally, eclipse PLD is used to successfully prepare efficient organic photovoltaic devices with ZnO:Ga top electrodes, which exhibit a similar performance compared to reference devices with state-of-the-art metal top contacts.

2. Results and Discussion

The performance of ZnO:Ga electrodes is strongly dependent on a variety of process parameters, e.g., laser intensity and pulse repetition rate, target composition, substrate material and temperature, residual gases in the vacuum chamber, and the pressure during deposition.[5,19] The optimized parameters, i.e., for deposition of a highly conductive and most transparent film at room temperature on standard glass substrates without organic films are: oxygen atmosphere at a pressure of 5×10^{-3} mbar, a pulse rate of 25 Hz, and an energy of 600 mJ per laser pulse. The transmittance spectrum and sheet resistance R_S of a ZnO:Ga (1 wt%) electrode, which is prepared under these conditions, are depicted in **Figure 2**a. In the visible spectral range between 400 and 800 nm, a mean transmittance T_{vis} of 82.5% (including the substrate) and an excellent R_S of 17.2 Ω sq^{-1} are achieved, emphasizing the great potential of gallium doped zinc oxide layers for transparent electrode applications.

However, under identical deposition conditions on an organic MH250 sublayer, the transmittance is drastically decreased to T_{vis} = 54% and the film is not conductive at all. The reason is well visible in the two SEM images of Figure 2b. On glass, the ZnO:Ga film forms a smooth, partially nanogranular microstructure, typical for pulsed laser deposition of ZnO at room temperature, which enables a high electrical conductivity and optical transmission. In contrast, a very rough surface is obtained on the organic material, such that the ZnO:Ga layer bursts and peels off. The multitude of tortuous cracks causes significant scattering and absorption of light, hinders an efficient charge transport, and thus explains the low film transmittance and conductivity. Even by eye, the electrode on top of MH250 looks milky and rough. Cracks in the layer are also indicated by the increased transmittance below 400 nm wavelength, above the energy gap of ZnO:Ga. Most likely, the energy input of the ablated ZnO:Ga particles during deposition into the sublayer is too high, "burning" the organic material and changing its morphology. Another possibility is that the soft organic material and the ZnO:Ga film are strained against each other during deposition and the stress release leads to a bursting surface. To reduce the energy of the arriving ZnO:Ga particles, the oxygen pressure in the chamber is gradually increased to 5×10^{-2} and 5×10^{-1} mbar, respectively. Thereby, the scattering probability of zinc oxide particles on gas atoms during transfer and their thermalization within the expanding plasma is enlarged.

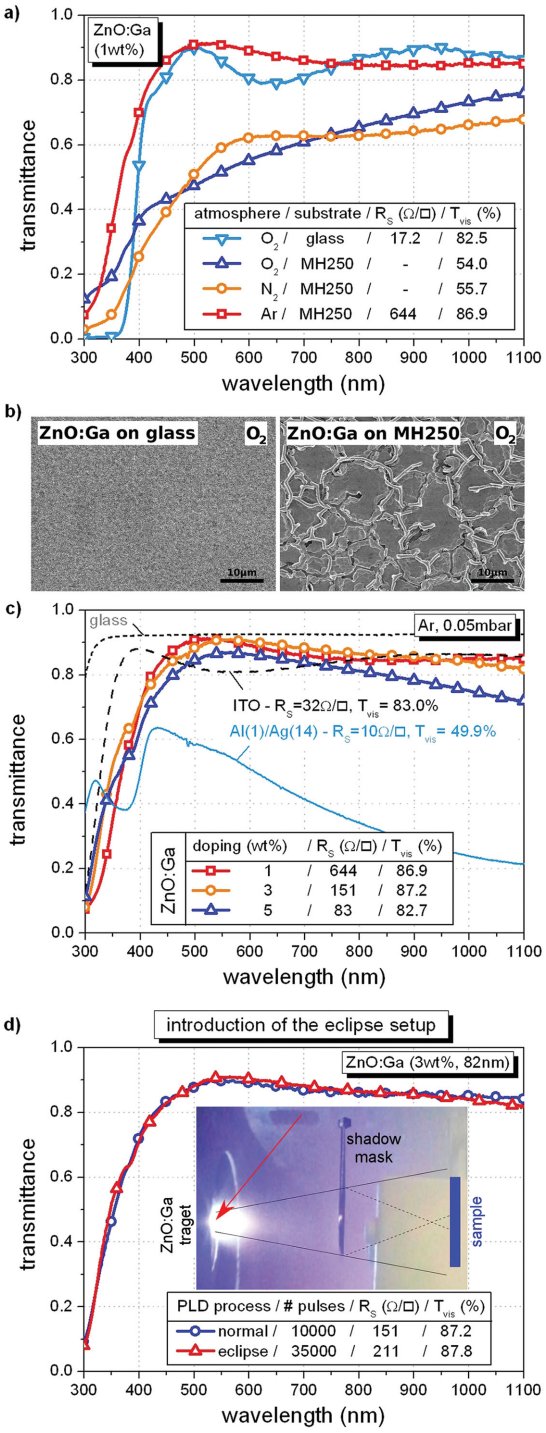

Figure 2. Electrode-only investigations: a) Transmittance spectra, mean visible transmittance T_{vis}, and sheet resistance R_S of ZnO:Ga (1 wt%) films on different substrates and for deposition in different background gas atmospheres (O_2, N_2, Ar). b) SEM images of O_2 atmosphere prepared ZnO:Ga films, deposited simultaneously on glass or organic MH250 surfaces. c) Optoelectronic performance of ZnO:Ga depending on the doping concentration as well as comparison to ITO and metal electrode references. d) Comparison of T_{vis} and R_S of two ZnO:Ga layers with identical thickness and doping concentration, which are prepared either by normal or eclipse PLD. The inset shows a photograph of the running eclipse PLD setup in which the sample is hidden behind a cover lid.

Indeed, the ZnO:Ga films deposited at higher pressures exhibit a smoother microstructure and an improved transmittance, but are still nonconductive (see Figure S2, Supporting Information, for more details). Probably too many oxygen interstitials and/or Zn vacancies reduce the conductivity of the ZnO.[20,21] Note that the laser ablation itself is almost not affected by the increased pressure in the deposition chamber, but the corresponding layer thickness is reduced.

Since oxygen atmosphere is known to degrade organic devices, the residual gas in the chamber is changed to nitrogen. The oxygen in ZnO can be partially released or replaced by nitrogen, leading to a strongly decreased electron mobility.[5] For ZnO:Ga films on MH250 sublayers deposited in nitrogen, similar transmittance spectra (T_{vis} = 55.7%) as in oxygen atmosphere are observed, but the layers remain nonconductive, although the crack formation is reduced. Instead, the films are of brownish color, suggesting an unfavorable material composition.

After further variation of the process gases, pressures, and layer thickness, a deposition of ZnO:Ga (1 wt%) in argon atmosphere at 5×10^{-2} mbar yielded layers of excellent mean optical transmission of 86.9% and a reasonable R_S of 644 Ω sq^{-1} even on the organic MH250 sublayer. Probably, the thermalization of ZnO:Ga particles in Ar is improved, leading to a uniform microstructure of the layer without cracks. With Ar background atmosphere the transmittance onset of ZnO:Ga films is significantly blue-shifted, caused by the shift of the absorption edge due to the Burstein Moss shift.

The conductivity of the ZnO:Ga electrode can be significantly improved by an increased concentration of Ga. Figure 2c shows the sheet resistance and transmittance of ZnO:Ga films (≈80 nm thick) on MH250, deposited in Ar (5×10^{-2} mbar) from different targets with doping concentrations of 1, 3, and 5 wt%. While at 1 wt% Ga a rather high sheet resistance of 644 Ω sq^{-1} is measured, R_S is strongly reduced to 151 Ω sq^{-1} and even 83 Ω sq^{-1} for 3 and 5 wt% doping, respectively. At the same time, the transmittance is slightly enhanced from 86.9% to 87.2% for the increase to 3 wt% doping. The introduction of more than 3 wt% Ga leads to an increased light absorption and the transmittance decreases to T_{vis} = 82.7% for the 5 wt% sample. The spectral shape is changed only slightly with doping. For comparison, the transmittance and sheet resistance of our lab ITO and a state-of-the-art metal top electrode comprising 1 nm of Al and 14 nm of Ag are plotted in Figure 2c. The Al/Ag bilayer exhibits, as it is typical for metal films, a very low R_S of 10 Ω sq^{-1}, but the transmittance is limited to T_{vis} = 49.9%. To increase this transparency, the metal thickness would need to be reduced, which typically leads to discontinuous films and an abrupt total loss of conductivity.[8] ITO, the current benchmark in the field of transparent conductors, cannot be used as top electrode, but shows a very high T_{vis} of 83% at a R_S of only 32 Ω sq^{-1}. However, in the spectral range between 460 and 850 nm, where the photon flux of the sun has its maximum, the ZnO:Ga (3 wt%) electrode exceeds the transmittance of ITO by up to 10.1%, pointing out the tremendous potential of this electrode in combination with a solar cell.

To avoid plasma and particle damage to the organic device during deposition of the top electrode, the system is adapted for elicpse PLD.[22–25] It is known from literature and previous

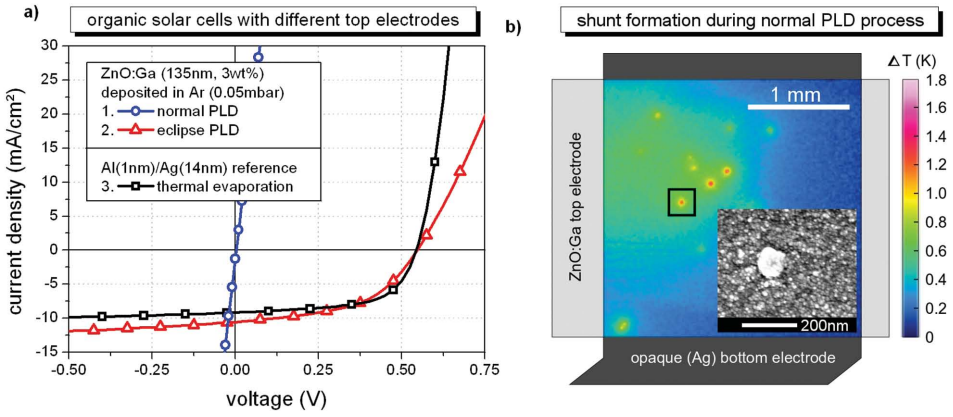

Figure 3. a) Current–voltage characteristics of solar cells with identical organic layer stack but different transparent top electrodes. While the ZnO:Ga electrodes are deposited by either normal or eclipse PLD in argon atmosphere with a base pressure of 0.05 mbar, the Al/Ag reference contact is deposited by thermal evaporation at 10^{-7} mbar. b) Thermograph top view of an organic solar cell with ZnO:Ga top electrode, which was prepared by normal PLD and operated at 10 mA under forward bias voltage. Local short circuits lead to the formation of several, statistically distributed hot-spots. The SEM image of a characteristic hot-spot reveals a round droplet with a diameter of around 100 nm.

investigations that inhomogeneities in the laser profile or in the composition of the ZnO:Ga target can cause a partial under-melting of the target material.[26] Thus, large and heavy particles—droplets—with high kinetic pulse and energy can detach from the target. In order to reduce a possibly negative influence of such droplets on the organic layers, a circular shadow mask (diameter of 19.4 mm) is installed between the target and the sample, as depicted in Figure 2d. Directly on the target, the laser generates a bright luminous plasma and from an ablation area of approximately 5 mm^2, a constant material flux is spread over a solid angle plume. The mask blocks all the ZnO:Ga particles flying straight to the sample. However, small particles in the expanding plasma plume can change their direction due to collisions with gas atoms and are significantly scattered during the thermalization process in the argon atmosphere of comparable high pressure (5×10^{-2} mbar). The eclipse PLD configuration still enables the deposition of a homogeneous film behind the shadow mask from such thermalized species, indicated by the dashed lines in Figure 2d. In contrast, heavy particles have much higher momentum, move along a straight line trajectory, and are successfully blocked by the mask or miss the sample. With such a mask, the deposition rate and layer thickness on the sample for a constant number of laser pulses is substantially decreased by a factor of 3.5, since a major part of the material is blocked. Consequently, the pulse number has to be increased to achieve a similar layer thickness. However, even if an identical layer thickness is realized, the sheet resistance of a ZnO:Ga (3 wt%, 82 nm) electrode increases from 151 Ω sq^{-1} (normal PLD) to 211 Ω sq^{-1} (eclipse PLD) as shown in Figure 2d. This can be only explained by a material specific resistivity increase, suggesting a slightly less favorable ZnO:Ga morphology for eclipse preparation, caused by the lower energy of the impacting particles at the substrate surface.[27] The excellent optical properties of the electrode are not affected. In summary, argon at a base pressure of 5×10^{-2} mbar is identified as a suitable ambient for the preparation of highly transparent and conductive ZnO:Ga electrodes on top of organic materials, either by comparably fast standard PLD or gentle eclipse PLD.

To investigate the device applicability, 135 nm thick ZnO:Ga (3 wt%) electrodes are finally deposited on top of complete organic photovoltaic cells. The corresponding sheet resistance and transmittance spectrum can be found in Figure S1 of the Supporting Information. The specific layer thickness of 135 nm was selected from optical transfer matrix simulations[28] and represents an optimum for the field distribution in the solar cell stack. Figure 1 depicts the detailed OPV stack design. The current–voltage curves of the solar cells with ZnO:Ga top electrode under illumination are shown in **Figure 3**a and the corresponding characteristic parameters are summarized in **Table 1**. Standard pulsed laser deposition of the ZnP:Ga top electrode leads to a low series resistance (R_{series}) of only 27.1 Ω, comparable to the 20.5 Ω of the reference device with thin metal electrode. However, the steep and straight *IV*-curve, a poor fill factor (FF) of 25.0%, and an open circuit voltage (V_{OC}) of 0 *V* indicate a short circuit formation, leading to an efficiency of $\eta = 0$ %. Unfortunately, total device failure was observed independent of the ZnO:Ga thickness (20–200 nm) and doping concentration (1–5 wt%), if standard PLD is used.

In contrast, the reference device with simultaneously prepared organic stack and immediately deposited Al/Ag/Alq_3 top electrode does not exhibit such malfunction. It reaches a power conversion efficiency of η = 3.0% and all characteristic parameters behave like expected from other experiments on similar stacks.[29] The short circuit current density of the reference device J_{SC} = 9.1 mA cm^{-2} is limited by the moderate transmittance of the metal electrode (T_{vis} = 49.9%). But the V_{OC} of 0.54 V and a FF of 61.2% are excellent values for a ZnPc:C60 cell,[30,31]

Table 1. Characteristic parameters of identical solar cells with different transparent top electrodes.

#	Top electrode material	Deposition method	V_{OC} [V]	J_{SC} [mA cm^{-2}]	FF [%]	R_{series} [Ω]	η [%]
1	ZnO:Ga	Normal PLD	0	1.3	25.0	27.1	0
2	ZnO:Ga	Eclipse PLD	0.55	10.6	50.0	117	2.9
3	Al/Ag	Thermal evap.	0.54	9.1	61.2	20.5	3.0

proofing the functionality of the OPV stack and hinting on an incompatibility of standard PLD and organic sublayers. To obtain a better insight into the short circuit formation, thermography and SEM investigations of the solar cells with standard PLD ZnO:Ga top electrode are shown in Figure 3b.

At the position of local shunts, the current density of an operating device is particularly high, leading to stronger heating compared to the surrounding area. Thus, the current driven heating (at 10 mA in forward bias for 30 s) and cooling (at 0 mA for 30 s) of the complete solar cell area is visualized as false color temperature differential (ΔT) plot. Several hot-spots are observed, which are statistically distributed over the device area. Supplementary SEM images reveal droplets in the center of such hot-spots with particle sizes of 50 to 500 nm. Obviously, these large particles with high kinetic energy can pierce the entire organic stack and form the local shunts. However, not all droplets lead to short circuit formation.

After droplets are identified as reason for the total device failure, a series of attempts to protect the organic stack were investigated. Increasing the target-substrate distance further was not possible since the maximum target-substrate distance of that chamber was already used and further increase is probably not very useful, as the droplets move on straight line trajectories. The MH250 layer thickness was increased from 40 up to 260 nm with the aim to stop the droplets inside the soft ETL and prevent damage to the OPV stack. Furthermore, WO_3 layers with strong covalent bondings instead of weak van der Waals forces between organic molecules have been introduced on top of the organic stack to provide a higher mechanical resistance against the droplet penetration.[29] However, no trend towards a reduction of local short circuits has been observed for either approach. Finally, only eclipse PLD was able to block the critical droplets sufficiently. The best trade-off between droplet shielding, sample preparation time, and most important the device performance was achieved for a mask diameter of 19.4 mm, a target-mask distance of 50 mm, and a mask-sample distance of 72 mm, which were selected for the solar cell preparation.

As depicted in Figure 3a, the device with transparent ZnO:Ga top electrode, produced by eclipse PLD, shows a similar performance compared to the reference device in Figure 3a. The eclipse mask can sufficiently shield the entire solar cell area and no short circuits are observed. A V_{OC} of 0.55 V and no *S*-kink formation indicate a barrier-free charge extraction from the n-doped organic electron transport material MH250 into the ZnO:Ga electrode. Due to the excellent transmittance of the ZnO:Ga layer, a significantly improved short circuit current density of 10.6 mA cm^{-2} is achieved compared to 9.1 mA cm^{-2} of the reference device. However, the conductivity of ZnO:Ga is lower than that of the metal reference electrode. Thus, the series resistance of 117 Ω is much higher and FF = 50% is considerably lower for the ZnO:Ga solar cell than the 20.5 Ω and 61.2% of the metal reference. However, the organic solar cell with ZnO:Ga top electrode still exhibits an efficiency of $\eta = 2.9\%$, which is very close to $\eta = 3.0\%$ of the reference device with thin metal electrode, rendering the ZnO:Ga a suitable, new, and low-cost top electrode material. By our experiments, we could prove eclipse PLD is capable of depositing metal oxide materials onto sensitive organic thin films and therefore open new ways of combining the two material classes for innovative semiconductor devices.

3. Conclusion

For the first time, gallium doped zinc oxide has been successfully introduced as alternative transparent top electrode for organic solar cells. Under standard coating conditions, the ZnO:Ga films on top of organic material exhibit a poor microstructure and cause strong impact damage to the organic layers by high energy ZnO:Ga particles during deposition. Frequent cracks in the ZnO:Ga film and isolated ZnO:Ga microflakes cause strong light scattering, a low transmittance, and low conductivity. With eclipse PLD in argon atmosphere, a compatible, nonharmful deposition technique was identified, allowing the preparation of highly transparent (T_{vis} = 82.7%) electrodes with considerable sheet resistance (R_S = 83 Ω sq^{-1}) on top of organic material. With a σ_{dc}/σ_{ac} ratio of 77.3,[32] the eclipse PLD ZnO:Ga film is in the range of other transparent electrode systems typically used for optoelectronic devices. Organic photovoltaic cells prepared with this ZnO:Ga electrode obtained a similar efficiency (η = 2.9%) as a reference sample using a state-of-the-art metal top contact (η = 3.0%). Moreover, there is still room for an electrode improvement, considering further optimization of layer thickness, deposition rate, and doping concentration. In summary, with a well adjusted eclipse PLD process, we have combined the benefits from metal oxide electrodes and organic thin films for innovative semiconductor devices.

4. Experimental Section

All organic and metal layers of the samples shown in this publication were manufactured in a custom-made vacuum system (K.J. Lesker, UK) at IAPP by thermal (co-)evaporation at a base pressure of 10^{-8} mbar and using shadow masks. Glass (Corning Eagle XG, 1.1 mm, Thin Film Devices, USA) was used as substrate to guarantee reliable handling and sample processing. It was carefully cleaned with NMP, ethanol, and oxygen plasma before being transferred into the vacuum chamber. During one processing run of 18 samples in parallel, all layers were deposited under identical conditions. This allowed to include reference samples for direct comparison within the run, and also run to run comparisons to validate processing over time. All layer thicknesses were monitored by calibrated quartz crystal microbalances. The vacuum chamber was connected to a nitrogen glovebox, to guarantee reliable and save sample storing, packaging, and encapsulation under inert conditions.

The small molecule organic solar cells presented here were single-junction p–i–n type, i.e., the intrinsic absorber materials (i) were embedded between charge carrier selective, doped, and transparent electron (n) and hole (p) transport materials. The complete stack is shown in Figure 1. Since the focus of our investigation was the application of ZnO as top electrode, we decided to use standard organic materials in a simple and low-cost single-junction solar cell architecture, which was not able to achieve the cited record efficiency of 12%. However, this stack was well understood, reliable, and stable during the required sample transport (see below). Furthermore, we were convinced that with a higher budget and amore experimental effort, the presented results for the ZnO top electrodes could be realized on more efficient devices as well. As bottom electrode, an opaque and highly reflective silver (Ag) layer of 100 nm was used, creating a cavity in the device (indicated by the dashed lines) which enabled improved light absorption.

For efficient hole transport, 30 nm of *N*,*N*′-((diphenyl-*N*,*N*′-bis)9,9,-dimethylfluoren-2-yl)-benzidine (BF-DPB, Sensient AG, USA) doped with 10 wt% NDP9 (Novaled AG, Germany) were deposited, followed by 5 nm of intrinsic zinc-phthalocyanine (ZnPc, TCI EUROPE N.V., Belgium; purified by CreaPhys GmbH, Germany). A good charge carrier extraction and formation of an Ohmic contact was achieved by deposition of 1 nm pure NDP9 at the interface between silver and BF-DPB. Next, a 30 nm thick bulk heterojunction consisting of simultaneously evaporated C60 (BuckyUSA, USA; purified by CreaPhys GmbH, Germany) and ZnPc in a ratio of 1:1 was deposited as absorber layer, followed by 30 nm of intrinsic C60. As electron transport layer, 40 nm of *N*,*N*-Bis(fluoren-2-yl)-naphthalenetetracarboxylic diimide (MH250, produced in house) n-doped by 7 wt% of Tetrakis(1,3,4,6,7,8-hexahydro-2H-pyrimido[1,2-a] pyrimidinato)ditungsten (II) (W2(hpp)4, Novaled AG, Germany) was used. All organic materials except the dopants had been purified at least twice by vacuum gradient sublimation and were tracked in our material and processing database to ensure consistent material quality for all experiments.

The transparent ZnO:Ga top electrodes (135 nm thickness, 3 wt% doping concentration) were deposited in one of the medium-size PLD chambers of the semiconductor group at the Universität Leipzig. This electrode showed a mean transmittance of 86.5% and a sheet resistance of 144 Ω sq^{-1} (see Figure S1, Supporting Information). The chamber could be purged with pure oxygen, nitrogen, or argon to realize a specific background gas atmosphere during the deposition process with typical deposition pressure of 10^{-4} to 10^{-1} mbar. A krypton fluoride laser (LPX300, Lambda Physik, Germany) with a wavelength of 248 nm, a pulse rate between 1 and 50 Hz (we used 25 Hz in the present study), and an energy of 600 mJ per pulse was focused on a rotating ZnO:Ga target. Due to the target rotation homogeneous material ablation was achieved. The target-substrate distance of 120 mm guaranteed a sufficient thermalization of the ZnO:Ga particles (for the above mentioned gases and pressures) in the PLD chamber, before they reached the sample and allowed deposition on large substrates (here up to 3 in. For optimized eclipse PLD, a circular shadow mask with a diameter of 19.4 mm was installed, 70 mm in front of the sample and directly in the trajectory of the ablated ZnO:Ga particles (see inset of Figure 2d). In ref. [33], the PLD setup is described in detail.

As reference top electrode, a semitransparent state-of-the-art metal contact comprising 1 nm of aluminum (Al) and 14 nm of silver (Ag) was deposited in the vacuum system at IAPP. Al acted as protection layer against interdiffusion of Ag and organic material as well as seed layer for improved Ag thin film morphology.[6,7,34] Additionally, a 45 nm thick Alq_3 layer was used as capping layer, to reduce the reflectivity of the metal film.

Before the final PLD process was carried out, organic solar cells without top contact were transported from Dresden to Leipzig in a pre-baked KF36 vacuum tube under inert nitrogen atmosphere and normal pressure. Since the PLD chamber was not connected to a glovebox, the organic devices were fitted to the chamber under ambient conditions. A degradation of the organic materials or a reduced device performance due to the sample transport and temporary air exposure could be excluded, because of extensive and careful reference sample investigations. In fact, OPV cells with Al/Ag top contact, which were prepared in one step without breaking the vacuum, showed an identical efficiency as reference cells transported to Leipzig and back to Dresden without top contact. These samples were exposed to air (≈10 min) and the atmosphere in the PLD chamber (≈30 min, no deposition) for similar times as the samples on which a ZnO:Ga electrode was fabricated. Finally, on these references the same Al/Ag top electrodes were realized after being transported back to the IAPP again in the KF36 vacuum tube under inert nitrogen atmosphere and normal pressure. All completed devices were encapsulated at IAPP with a transparent encapsulation glass, fixed by UV-hardened epoxy glue (UV RESIN XNR5590, Nagase ChemteX, Japan), in a nitrogen glovebox. The photoactive area of the solar cells, resulting from the overlap of bottom and top electrode, is 2.54×2.54 mm^2.

To guarantee reliable results, we used a standard stack design which was frequently reproduced also in other experiments.[29–31] All materials were tracked in a material and processing database to ensure consistent quality for all experiments. Moreover, each sample presented in this paper was prepared four times under identical conditions. Except the eclipse PLD solar cells, all electrode-only samples and solar cells show process- and measurement-related relative deviations between these four identical samples of <3% for all relevant parameters. Thus, we stated only the average values. For our solar cells using eclipse PLD as top electrode deposition methode, larger deviations were observed, most likely due to the statistical process of droplet formation. The stated eclipse PLD device parameters are mean values of the two best samples.

Current–voltage measurements of the solar cells were carried out using a source measurement unit (2400 SMU, Keithley, USA) and simulated AM 1.5G sun light (16S-150V.3 by Solar Light Co., USA) taking spectral mismatch into account. The illumination intensity was kept at (100 ± 1) mW cm^{-2}, monitored by a calibrated silicon reference diode. To determine the external quantum efficiency (EQE) and the mismatch factor, a custom-made setup was used. The monochromatic beam (Oriel Xenon Arc-Lamp Apex Illuminator combined with Cornerstone 260 1/4m monochromator, both Newport, USA) probing the device was chopped and the corresponding current response of the device was measured via a lock-in amplifier 7265 DSP (Signal Recovery, UK). Local temperature differences on operating organic solar cells, e.g., because of local shunts, have been measured with a VarioTherm InSb (InfraTec, Germany) infrared camera. It detected thermal radiation in the range of 2 to 5 µm wavelength with a resolution of 640 × 512 pixels and allows a precision of ±0.1 K. Since the local short circuits were assumed to be smaller than the pixel resolution (one pixel can image 4 × 4 µm 2 on the sample), the measured temperature differences were average values for each pixel area and could be significantly lower than the actual temperature in a local hot spot. However, by comparing images of a solar cell with and without external bias current, even small shunts could be detected.

Additionally, the ZnO:Ga and Al/Ag electrodes are deposited on simpler substrates, which use only one layer of n-doped MH250 (40 nm, 7 wt%) on glass, and are characterized by optical and electrical studies. The MH250 is exactly the same material below the deposited electrode layer as it is used in the solar cell. Thus, the growth of oxide and metal is decoupled from the glass substrate and exhibits similar growth conditions as on top of the complete organic device. These electrode-only samples are used to optimize the ZnO:Ga layer performance by a systematical variation of layer thickness (20–200 nm), background gas atmosphere (O2, N2, Ar) and base pressure (from 10^{-4} to 10^{-1} mbar) during deposition, as well as doping concentration (1–5 wt%). Not all variations were discussed in this article, as we focused on the more promising results. The transmittance of these electrodes is recorded using an Ava-Light-DH-S-Bal (Avantes BV, Netherlands) light source and a CAS 140 CT spectrometer (Instrument Systems GmbH, Germany) through an aperture of 2.96 mm^2. A four-point-probe measurement stand S 302–4 (LucasLabs, USA) was used to determine sheet resistances under ambient conditions. Scanning electron micrographs of the ZnO:Ga films were recorded using a Zeiss GSM 982 Gemini scanning electron microscope (SEM). Several measurements were recorded at different positions to ensure reproducible results that actually represent the entire sample.

Supporting Information

Supporting Information is available from the Wiley Online Library or from the author.

Acknowledgements

This work was in part funded by the Bundesministerium für Bildung und Forschung in the framework of the InnoProfile project (03IP602). Also support from the excellence cluster cfaed is gratefully acknowledged. The authors thank Andreas Wendel and Tobias Günther from IAPP as well

as Holger Hochmuth and Prof. Michael Lorenz from the semiconductor group in Leipzig for assistance with sample preparation. Additionally, the authors thank Susanne Goldberg from TU Dresden for the SEM measurements and Jacqueline Brückner from Fraunhofer Comedd (now FEP) for the thermographs.

Received: February 10, 2015
Revised: April 13, 2015
Published online: June 5, 2015

[1] A. Anctil, C. W. Babbitt, R. P. Raffaelle, B. J. Landi, *Prog. Photovoltaics* **2013**, *21*, 1541.
[2] Heliatek: Neuer Weltrekord für organische Solarzellen, www.heliatek.com (accessed: August **2014**).
[3] H. Kim, C. M. Gilmore, A. Pique, J. S. Horwitz, H. Mattoussi, H. Murata, Z. H. Kafafi, D. B. Chrisey, *J. Appl. Phys.* **1999**, *86*, 6451.
[4] A. Feltrin, A. Freundlich, *Renewable Energy* **2008**, *33*, 180.
[5] C. G. Granqvist, *Sol. Energy Mater. Sol. Cells* **2007**, *91*, 1529.
[6] J. Meiss, M. Riede, K. Leo, *J. Appl. Phys.* **2009**, *105*, 063108.
[7] S. Schubert, J. Meiss, L. Müller-Meskamp, K. Leo, *Adv. Energy Mater.* **2013**, *3*, 344.
[8] J.-Y. Lee, S. T. Connor, Y. Cui, P. Peumans, *Nano Lett.* **2010**, *1*, 9721.
[9] J. Krantz, T. Stubhan, M. Richter, S. Spallek, I. Litzov, G. J. Matt, E. Spiecker, C. J. Brabec, *Adv. Funct. Mater.* **2013**, *23*, 1711.
[10] F. Selzer, N. Weiß, D. Kneppe, L. Bormann, C. Sachse, N. Gaponik, A. Eychmüller, K. Leo, L. Müller-Meskamp, *Nanoscale* **2015**, *7*, 2777.
[11] Y.-H. Kim, L. Müller-Meskamp, A. A. Zakhidov, C. Sachse, J. Meiss, J. Bikova, A. Cook, A. A. Zakhidov, K. Leo, *Solar Energy Mater. Solar Cells* **2012**, *96*, 244.
[12] P. Lin, W. C. H. Choy, D. Zhang, F. Xie, J. Xin, C. W. Leung, *Appl. Phys. Lett.* **2013**, *102*, 113303.
[13] S. Schubert, Y. H. Kim, T. Menke, A. Fischer, R. Timmreck, L. Müller-Meskamp, K. Leo, *Solar Energy Mater. Solar Cells* **2013**, *118*, 165.
[14] G. Gu, V. Bulovic, P. E. Burrows, S. R. Forrest, M. E. Thompson, *Appl. Phys. Lett.* **1996**, *68*, 2606.
[15] H. K. Kim, D. G. Kim, K. S. Lee, M. S. Huh, S. H. Jeong, K. I. Kim, T. Y. Seong, *Appl. Phys. Lett.* **2005**, *86*, 183503.
[16] H. Kim, J. S. Horwitz, W. H. Kim, A. J. Mäkinen, Z. H. Kafafi, D. B. Chrisey, *Thin Solid Films* **2002**, *420*, 539.
[17] R. C. Scott, K. D. Leedy, B. Bayraktaroglu, D. C. Look, D. J. Smith, D. Ding, X. Lu, Y.-H Zhang, *J. Electron. Mater.* **2011**, *40*, 419.
[18] H. Yamamoto, T. Oyamada, W. Hale, S. Aoshima, H. Sasabe, C. Adachi, *Jpn. J. Appl. Phys.* **2006**, *45*, 213.
[19] Y. C. Lin, T. Y. Chen, L. C. Wang, S. Y. Lien, *J. Electrochem. Soc.* **2012**, *159*, 599.
[20] S. Pearton, D. Norton, K. Ip, Y. Heo, T. Steiner, *Prog. Mater. Sci.* **2005**, *50*, 293.
[21] F. Oba, M. Choi, A. Togo, I. Tanaka, *Sci. Technol. Adv. Mater.* **2011**, *12*, 034302.
[22] K. Kinoshita, H. Ishibashi, T. Kobayashi, *Jpn. J. Appl. Phys.* **1994**, *33*, 417.
[23] M. Tachiki, M. Noda, K. Yamada, T. Kobayashi, *J. Appl. Phys.* **1998**, *83*, 5351.
[24] M. Sugiura, K. Uragou, M. Noda, M. Tachiki, T. Kobayashi, *Jpn. J. Appl. Phys.* **1999**, *38*, 2675.
[25] S. Müller, H. von Wenckstern, F. Schmidt, D. Splith, R. Heinhold, M. Allen, M. Grundmann, *J. Appl. Phys.* **2014**, *116*, 194506.
[26] M. Lorenz, in *Transparent Conductive Zinc Oxide* (Eds: K. Ellmer, A. Klein, B. Rech), Springer, Berlin **2008**, pp 303–357.
[27] J. A. Sansa, A. Seguraa, J. F. Sánchez-Royoa, V. Barbera, M. A. Hernández-Fenollosab, B. Maríb, *Superlattices Microstruct.* **2006**, *39*, 282.
[28] L. A. A. Pettersson, L. S. Roman, O. Inganäs, *J. Appl. Phys.* **1999**, *86*, 487.
[29] S. Schubert, M. Hermenau, J. Meiss, L. Müller-Meskamp, K. Leo, *Adv. Funct. Mater.* **2012**, *22*, 4993.
[30] S. Pfützner, C. Mickel, J. Jankowski, M. P. Hein, J. Meiss, C. Schuenemann, C. Elschner, A. A. Levin, B. Rellinghaus, K. Leo, M. Riede, *Org. Electron.* **2011**, *12*, 435.
[31] C. Schünemann, D. Wynands, L. Wilde, M. P. Hein, S. Pfützner, C. Elschner, K.-J. Eichhorn, K. Leo, M. Riede, *Phys. Rev. B* **2010**, *85*, 245314.
[32] L. Hu, D. S. Hecht, G. Grüner, *Nano Lett.* **2004**, *4*, 2513.
[33] M. Lorenz, H. Hochmuth, C. Grüner, H. Hilmer, A. Lajn, D. Spemann, M. Brandt, J. Zippel, R. Schmidt-Grund, H. von Wenckstern, M. Grundmann, *Laser Chem.* **2010**, 140976.
[34] S. Olthof, J. Meiss, M. Riede, B. Lüssem, K. Leo, *Thin Solid Films* **2011**, *519*, 1872.